ORIGINAL ARTICLE

Distribution of cell-wall polysaccharides and proteins during growth of the hemp hypocotyl

Marc Behr[1] · Claudia Faleri[2] · Jean-Francois Hausman[1] · Sébastien Planchon[1] · Jenny Renaut[1] · Giampiero Cai[2] · Gea Guerriero[1]

Abstract

Main conclusion The immuno-ultrastructural investigation localized cell-wall polysaccharides of bast fibers during hemp hypocotyl growth. Moreover, for the first time, the localization of a peroxidase and laccase is provided in textile hemp.

Abstract In the hypocotyl of textile hemp, elongation and girth increase are separated in time. This organ is therefore ideal for time-course analyses. Here, we follow the ultrastructural rearrangement of cell-wall components during the development of the hemp hypocotyl. An expression analysis of genes involved in the biosynthesis of cellulose, the chief polysaccharide of bast fiber cell walls and xylan, the main hemicellulose of secondary cell walls, is also provided. The analysis shows a higher expression of cellulose and xylan-related genes at 15 and 20 days after sowing, as compared to 9 days. In the young hypocotyl, the cell walls of bast fibers show cellulose microfibrils that are not yet compacted to form a mature G-layer. Crystalline cellulose is detected abundantly in the S1-layer, together with unsubstituted/low-substituted xylan and, to a lesser extent, in the G-layer. The LM5 galactan epitope is confined to the walls of parenchymatic cells. LM6-specific arabinans are detected at the interface between the cytoplasm and the gelatinous cell wall of bast fibers. The class III peroxidase antibody shows localization in the G-layer only at older developmental stages. The laccase antibody shows a distinctive labelling of the G-layer region closest to the S1-layer; the signal becomes more homogeneous as the hypocotyl matures. The data provide important insights on the cell wall distribution of polysaccharide and protein components in bast fibers during the hypocotyl growth of textile hemp.

Keywords *Cannabis sativa* L. · Hypocotyl · Bast fibers · Cell-wall polysaccharides · Electron microscopy

✉ Giampiero Cai
giampiero.cai@unisi.it

✉ Gea Guerriero
gea.guerriero@list.lu

1 Research and Innovation Department, Luxembourg Institute of Science and Technology, 5 Avenue des Hauts-Fourneaux, 4362 Esch/Alzette, Luxembourg

2 Department of Life Sciences, University of Siena, via P.A. Mattioli 4, 53100 Siena, Italy

Introduction

Textile hemp (*Cannabis sativa* L.) is a fiber crop typically found in the Northern hemisphere and grown specifically for industrial purposes. It is one of the fastest growing herbaceous species and was one of the first plants to be used for fiber production (Fike 2016). Hemp can be used in a variety of commercial products including paper, textiles, clothing, biodegradable plastic, canvas, biofuel, food and feed. Fibers can be used to produce cloths, usually mixed with other organic fibers such as linen, cotton or silk. Hemp fibers have been widely used throughout history, with a peak of production after being introduced into the New World. Currently, hemp fibers are mainly used in the textile and automotive industries (Andre et al. 2016).

The mechanical strength of hemp fibers is due to the presence of specialized cells (known as bast fibers), whose cell walls are enriched in cellulose (> 80%) and show high mechanical properties (Crônier et al. 2005; Roach et al. 2011; Guerriero et al. 2013). Bast fibers surround the xylem and are therefore defined as extraxylary fibers. Primary bast fibers derive from the procambium; in hemp, secondary bast fibers are generated by the cambium (Snegireva et al. 2015). Individual fibers are associated, by means of the middle lamella, to form fiber bundles parallel to the longitudinal axis of the stem, thus providing a mechanical support to the plant. At maturity, primary bast fibers can be several centimeters long with a diameter of about 20 μm. Secondary fibers are shorter (a few millimeters in length) and thinner than the primary bast fibers.

In hemp, as well as in flax, ramie and nettle, bast fibers are characterized by thick gelatinous cell walls (a.k.a. G-layer) (Gorshkova et al. 2018) composed of crystalline cellulose. These cell walls differ from xylan-type cell walls typically found in bast fibers of jute and kenaf (Mikshina et al. 2013; Guerriero et al. 2017). The mechanical properties of bast fibers are determined during the assembly of the macromolecules (polysaccharides, lignin, proteins) composing the different cell wall layers. This developmental process follows a precise temporal scheme consisting of primary cell wall (PCW) synthesis, followed by the development of the secondary (SCW) and G-layer. These latter are deposited according to a predetermined model, with the S1-layer being assembled first, followed by the progressive development of the G-layer. The composition of the S1-layer is similar to the xylan-type wall. In contrast, the G-layer has a quite different organization (Mikshina et al. 2013): it displays a high content of cellulose, the cellulose fibrils are axially oriented, it does not contain xylan nor lignin and is of considerable thickness (> 10 μm). The relative number of glucan chains in cellulose fibrils is four times larger in the G-layer than in the S1-layer (Mellerowicz and Gorshkova 2012). It must be noted that this G-layer shares some similarities with the cell wall of tension wood that are almost devoid of hemicellulose and lignin, but with a considerable proportion of non-cellulosic matrix polysaccharides (ca. 20%) (Mellerowicz and Gorshkova 2012). The proportion of the non-cellulosic polysaccharides (NCPs) found in the G-layer differs between species: xyloglucan and rhamnogalacturonan-I (RG-I) are, respectively, the major forms in poplar and flax. In flax, the major sugar of the G-layer pectin is galactose (55-85%), followed by rhamnose and galacturonic acid (Gorshkova and Morvan 2006). This polymer is characterized by a high degree of rhamnose branching and side chains of β-(1→4)-linked galactose of variable length and Gal:Rha ratio. This side chain is detected by the LM5 antibody (specific for relatively long 1→4-β-galactosyl residues, DP≥4), which displays a strong signal in the flax galactan-layer (Gn-layer) preceding the formation of the mature G-layer (Andeme-Onzighi et al. 2005; Gorshkova and Morvan 2006). As the Gn-layer matures, the LM5 signal decreases in intensity, pointing to a remodeling of the pectic galactan, resulting in the transition to the G-layer (His et al. 2001; Gorshkova and Morvan 2006; Roach et al. 2011; Hobson and Deyholos 2013).

The cell wall monosaccharide analysis of isolated bast fibers from flax hypocotyls suggests that pectins enrobing cellulose microfibrils are half polygalacturonic acid (PGA, the backbone of RG-II) and half RG-I, with an overall PGA-to-rhamnose ratio of around 6 (Andeme-Onzighi et al. 2005). The nature of the polysaccharides of hemp bast fibers is different from that of flax. For example, the LM5 signal found in flax (Andeme-Onzighi et al. 2005; Salnikov et al. 2008) is not observed in hemp (Blake et al. 2008; Behr et al. 2016). Hence, the structure of the main NCP of the Gn-layer is not the same. Most likely, the minimum of three sugar residues at the non-reducing end is not present (Andersen et al. 2016).

A detailed ultrastructural analysis on hemp bast fibers helps understanding how the G-layer is synthesized and remodeled. Two recent articles in the literature (Gorshkova et al. 2018; Kiyoto et al. 2018) have provided information in this respect, by focusing on a set of cell wall components. However, the ultrastructural mapping of crystalline cellulose, arabinans and galactans has not yet been performed on textile hemp, to the best of our knowledge.

We here analyzed, at an ultrastructural level, the distribution of key polysaccharides in bast fiber cell walls, using a series of antibodies widely cited in the literature (McCartney et al. 2005). We focused our attention on the chief components xylans, using the LM10 antibody binding to unsubstituted/low-substituted xylans, different from the LM11 previously used (Gorshkova et al. 2018) which recognizes also arabinoxylans in addition to unsubstituted xylans, as well as on crystalline cellulose. Additionally, we analyzed galactans, RG-I, arabinans and, for the first time, a hemp laccase and peroxidase, two classes of proteins involved in lignification (Novo-Uzal et al. 2013; Schuetz et al. 2014).

We here use the hemp hypocotyl as a model for two reasons. First, we previously proved that it is a good system to follow the changes in expression of genes related to cell wall formation during the transition from primary to secondary growth (Behr et al. 2016). Second, the hypocotyl completes its development within 3 weeks and grows more homogeneously than adult hemp plants. The sampling of homogeneous material for molecular studies is an issue when working with varieties and not clones. Therefore, although not being the tissue from which bast fibers are extracted, the hemp hypocotyl provides important and representative information on the cell wall organization of these cells. The analysis was performed at different developmental stages of the hemp hypocotyl, more specifically at 9, 15, and 20 days after

sowing, which characterize the stages of active elongation (until day 9) and secondary growth (at 15 and 20 days).

Materials and methods

Cultivation of plants of *Cannabis sativa*

Plants of *Cannabis sativa* (cultivar Santhica 27) were cultivated as previously described (Behr et al. 2016). Sampling was carried out by cutting the hypocotyls from plantlets aged 9, 15, and 20 days (hereafter referred to as H9, H15, and H20, respectively). Three independent plantlets were sampled per time-point analyzed.

RT-qPCR

Total RNAs from whole hypocotyls at H9–H15–H20 were extracted (in biological triplicate) and quality-checked as already described (Behr et al. 2016). RT-qPCR analyses were performed in 384-well plates on a ViiA7 Real-Time PCR System (Applied Biosystems) with the Takyon SYBR Green low ROX (Eurogentec). The primers were designed and validated as described (Behr et al. 2018a) and the primer list can be found in the same manuscript. The sequences used for primer design are given in Supplementary Document S1. The specificity of the amplification was checked with a melt curve at the end of each run. Relative gene expressions were determined with qBASE$^+$ (Biogazelle) using *CsaET-IF4e* and *CsaGAPDH* as reference genes (identified as the most stable and enough for correct normalisation among *Histone*, *EF2*, *Actin*, *Cyclophilin*, *Ubiquitin*, *GAPDH*, *Tubulin*, *ETIF4E*, *ETIF3H,* and *ETIF3E*). The one-way ANOVA and Tukey post hoc tests were performed to assess the differences between the groups.

Preparation of samples for electron microscopy

All samples were fixed with 3% glutaraldehyde in cacodylate buffer for 2 h at room temperature and at 4 °C overnight. After washing in cacodylate buffer (3 times for 15 min each), samples were post-fixed in 1% OsO4 for 1 h at room temperature. Following several washes in water (at least 3 times for 15 min each), samples were stored in water until dehydration in a graded series of ethanol: 10% EtOH for 5 min, 30% EtOH for 10 min, 50% EtOH for 15 min and 70% EtOH for storage. After dehydration, sections were included in SPURR resin for ultrastructural analysis. Ultrafine sections were obtained with a diamond knife in the ultramicrotome LKB NOVA, collected on a grid and stained for 20 min with 2% uranyl acetate and for 5 min with lead citrate at room temperature (Reynolds 1963).

Preparation of samples for immuno-electron microscopy

Hypocotyls of hemp were sectioned 1 cm below the cotyledons using a sharp razor blade. Hypocotyl sections (not more than 2 mm in thickness) were fixed for 2 h at room temperature and overnight at 4 °C in a mixture of 2% glutaraldehyde and 1.6% paraformaldehyde in 0.1 M phosphate buffer pH 6.9. Subsequently, samples were washed with phosphate buffer (2×10 min), then dehydrated in a series of absolute ethanol at the following percentages: 10% for 5 min, 30% for 10 min, 50% for 15 min, 70% for 30 min, 100% for 1 h (with a change every 20 min). Samples were infiltrated with LR-White resin in the following ratio with ethanol: 1:1 resin:ethanol for one night, 3:1 resin:ethanol for 1 day, pure resin for 1 day. Polymerization of the resin was carried out for 2 days at 40 °C. Ultrafine sections were obtained with a diamond knife in the ultramicrotome LKB NOVA.

Antibodies and immunolabelling

For immuno-localization, hypocotyl sections at different developmental stages were collected on gold grids and blocked for 20 min with normal goat serum (NGS) diluted 1:30 in dilution buffer (0.05 M Tris–HCl pH 7.6, 0.9% NaCl and 0.2% BSA); sections were incubated for 4 h at room temperature with primary antibodies LM5 [specific for (1-4)-β-D-galactan, catalogue no. LM5-050], LM6 (1,5-α-L-arabinan; LM6-050), LM10 (for xylan; LM10-050), INRA-RU1 (for rhamnogalacturonan I backbone) diluted 1:5 with dilution buffer. All antibodies were purchased from Plant-Probes (http://www.plantprobes.net). INRA-RU1 was kindly provided by Dr. Marie-Christine Ralet (INRA Angers-Nantes). Sections were then washed for 20 min in the dilution buffer + 0.1% Tween 20 and incubated for 45 min at room temperature with 10 nm gold particle-conjugated anti-rat secondary antibodies diluted 1:20 in 0.02 M Tris–HCl pH 8.2. To visualize crystalline cellulose, the CBM3a protein was used at a concentration of 5 μg/ml for 1.5 h combined with mouse monoclonal anti-His antibody diluted 100 times in dilution buffer + 0.1% Tween 20 for 1.5 h. Samples were washed and then incubated with the anti-mouse antibody conjugated with 10 nm gold particles for 45 min at room temperature. All sections were examined with the Philips MORGAGNI 268 80 kV transmission electron microscope, equipped with MEGAview II camera and elaborated with the Analysis software.

The primary antibody PRX64 (against peroxidase) was used after 1:20 dilution for 3 h at room temperature, followed by incubation with anti-rabbit secondary antibodies conjugated with 10 nm-gold particles for 45 min at room temperature. This custom antibody was produced externally

(Eurogentec), by co-injecting in rabbit two different peptides designed on the protein corresponding to *CsaPRX64* (contig 11948) (Behr et al. 2016), an ortholog of enzymes involved in lignin polymerization in *A. thaliana*. A non-redundant sequence has been used to produce a polyclonal antiserum (CNKVKNAGTTLDSTST). The specificity of CsaPRX64 was checked by Western blotting (WB) on an extract of hemp cell wall proteins (Printz et al. 2015). To confirm the antigen, the proteins present in the extract were separated in duplicate with a 2D-gel. The pH range of the first dimension was 3–10 (nonlinear gradient, 11 cm strips), while the percentage of the second-dimension gel was 12.5%. The first 2D gel was used to perform, after transfer to a nitrocellulose membrane, a WB with the CsaPRX64 antibody. The primary antibody was diluted 1:1000 in 5% BSA (w/v) in 0.1% TBS-Tween 20 (incubation overnight at 4 °C), while the secondary antibody used for chemiluminescence detection was diluted 1:5000 in PBS-0.1% TBS-Tween 20 and allowed to incubate for 1 h at room temperature. Detection was performed after incubation with the Western Blot chemiluminescence reagents (Bio-Rad) for 5 min at room temperature. The second gel was stained with LavaPurple (Serva Electrophoresis GmbH) according to the manufacturer's instruction; the spots where a signal was detected with the 2D-WB were picked and identified by MALDI MS/MS (Behr et al. 2018b).

The anti-laccase antibody (Lac17) was used at a dilution of 1:30 for 3 h at room temperature followed by incubation with anti-rabbit secondary antibodies conjugated with 10 nm-gold particles for 45 min at room temperature. This custom antibody was produced by Eurogentec based on contig 9466 (Behr et al. 2016) (non-redundant sequence CGPNPNQKLPPPPSDL). We tested the specificity of the antibody by dot blot assay against the peptide used as immunogen. For control, the antibody was tested against crude protein extracts of stem and leaves of hemp. Extracts were prepared by precipitation with TCA-acetone (Behr et al. 2018b), followed by a solubilization in 80% PBS, 2% SDS and 1% protease inhibitor (GE Healthcare). The primary

antibody was diluted 1:1000 in 5% BSA (w/v) in TBS-Tween 20 0.05% (incubation overnight at 4 °C) while the secondary antibody, donkey anti-rabbit coupled with Alexa 680 (ref 175772, Abcam), used for fluorescence detection was diluted 1:10000 in TBS-Tween 20 0.05% and allowed to incubate for 1 h at room temperature. Detection was performed with a Typhoon FLA 9500 with the setting of Alexa 647 fluorescence. A list of antibodies used, their specificity and relevant references is provided in Table 1.

Image analysis

To get a quantitative distribution of gold particles, immunolocalization images were subjected to measurement of signal density. Images were imported into ImageJ and they were calibrated with the "Set Scale" command. Subsequently, images were subjected to threshold, so that only gold particles were highlighted. Using the "Straight line" command, a "line of interest" was drawn in the cell-wall regions where we wanted to measure particle density. The thickness of the line of interest was extremely broad (larger than 500 nm) to get more representative data. We usually analyzed 10 images per sample, and we made 3–4 measurements for each one. To compare results from different experiments, data were normalized so that the highest value of gray level was arbitrarily set to 100. All other values were changed accordingly.

Results

To ease the reading of the Results section, a first part centered on gene expression will be presented to show the major changes in the expression of xylan and cellulose biosynthetic genes during primary and secondary growth. As previously mentioned, xylan and cellulose are here considered as they are the key components of secondary tissues and compose the S1- and G-layer of bast fibers, respectively. Subsequently, the ultrastructural features of the developing hypocotyl will be described, together with the mapping of

Table 1 Targeted cell wall epitopes and corresponding antibodies

Antibody	Epitope	References
INRA-RU1	Rhamnogalacturonan-I (RG-I) backbone	Ralet et al. (2010)
LM5	(1-4)-β-D-Galactan (RG-I side chain)	Jones et al. (1997)
LM6	1,5-α-L-Arabinan (RG-I side chain)	Willats et al. (1998)
LM10	Nonreducing end of xylans	Ruprecht et al. (2017)
CBM3a	Crystalline cellulose, xyloglucan	Blake et al. (2006) and Hernandez-Gomez et al. (2015)
LAC17	Laccase, homolog of AtLAC17	This study
PRX64	Class III peroxidase, homolog of AtPRX64	This study

Note that CBM3a is a bacterial carbohydrate-binding module, not an antibody

xylan, crystalline cellulose, and pectic components. The high-resolution analysis will be complemented by the distribution of two proteins, i.e., a hemp class III peroxidase and a laccase.

Xylan- and cellulose-related genes are highly expressed at later stages of the hemp hypocotyl's development

We previously published an RNA-Seq analysis of the developing hemp hypocotyl (Behr et al. 2016). The data reveal the suitability of the hemp hypocotyl to study secondary growth and bast fiber development. Transcriptomics shows the upregulation of several genes important for glucuronoxylan biosynthesis between H9 and H20. We here summarize the expression of genes involved in xylan backbone elongation (*GUT1*, *GUT2*, *IRX14*, *IRX15-L*), glucuronic acid (GlcA) substitution (*FRA8*, *GUX2*, *GUX4*), GlcA methylation (*GXM3*), backbone acetylation (*ESK1*, *RWA3*) and biosynthesis of the xylan reducing-end sequence (XRES) (*FRA8*, *GAUT12*) (Lee et al. 2011; Hao and Mohnen 2014) (Fig. S2). All the genes show a statistically significant increase in expression between H9 and H15/H20.

Our previously-published RNA-Seq analysis highlighted also the upregulation of genes involved in the deposition of crystalline cellulose and, more in general, the assembly of the secondary cell wall (SCW). Indeed genes partaking in cellulose biosynthesis (SCW *CesA*s, i.e., *CesA4*, *CesA7*, *CesA8,* and *IRX6*), cellulose crystallization (*CTL2* and *COB*) (Sanchez-Rodriguez et al. 2012; Sorek et al. 2015) and SCW organization (*FLA11* and *FLA12*) (MacMillan et al. 2010) are significantly more expressed in H15 and H20, as compared to H9 (Fig. S3a). Since cellulose is the major component of bast fiber cell walls, a targeted qPCR was performed on both PCW and SCW *CesA*s, to show their different expression patterns during the development of the hypocotyl. The analysis confirms that the *CesA*s related to SCW formation are significantly upregulated in H15 and H20, in parallel with the upregulation of xylan biosynthetic genes, while no clear differences are observed for the *CesA*s expressed during PCW formation (*CesA1A*, *CesA1B*, *CesA3*, *CesA6A*, and *CesA6B*) (Fig. S3b). These genes show indeed a constant level of expression that is independent of the growth stage.

Major ultrastructural changes accompany the development of the hemp hypocotyl

The first step in the work consisted in the ultrastructural analysis of hemp bast fibers at different developmental stages. As expected, the three phases showed a progressive development of the SCW layers (Fig. 1a–c). While the developmental stage H9 is characterized by the presence of the S1-layer (from now on indicated with double empty arrows) and a thinner G-layer (from now on indicated with double filled arrows) (Fig. 1a), the next stages (H15 and H20, Fig. 1b, c) are specifically characterized by a considerable thickening of the G-layer. Also, the S1-layer is more electron-lucent at H9 and becomes more electron-dense as the hypocotyl ages. While the thickness of the S1-layer is constant during the transition from H9 to H20, the thickness of the G-layer increases from about 400 nm in the H9 stage to approximately 2 μm in the H20 stage. Higher magnification images at H9 clearly show a loose cell wall structure (which we call Gf, from "fibrillar") disclosing details of what most likely are cellulose fibers at the initial developmental stages (Fig. 1d) and not yet forming a mature, more compact and homogeneous G-layer. At H20, an additional layer is present between the G-layer and the cell cytoplasm (presumably transitory, indicated by dotted double arrow), which likely coincides with the "stripped" Gn-layer of the cell wall (Chernova et al. 2018) (Fig. 1c, e). At H20, the G-layer is more compact and homogeneous, while the Gn-layer appears still fibrillar (Fig. 1e).

Ultrastructural localization of the pectic epitopes galactans, rhamnogalacturonan and arabinans

Galactans are galactose-containing polymers involved in the structuring of SCWs in bast fibers (Gorshkova et al. 2004; Gorshkova and Morvan 2006). In this work, we analyzed the distribution of galactans using the LM5 antibody. At H9, the immunogold signal is found in the cell walls of parenchyma cells (arrowheads, Fig. 2a). At the same developmental stage, the signal in the bast fibers is very weak (Fig. 2b), if not absent. Neither the S1- nor the G-layer of bast fibers show labelling with the LM5 antibody. At H15, the bast fibers do not show any signal (Fig. 2c). The cell wall of parenchyma cells is instead uniformly labelled (Fig. 2d, e). The distribution of the LM5-labelled epitopes is also unchanged at H20. In addition, the immunolabelling signal is again noticeably clear in the cell wall of parenchyma cells (arrowhead, Fig. 2f, g), but absent in the cell walls of bast fibers.

Due to the lack of an LM5 signal and to have more information on the distribution of pectic RG-I, a labelling was performed with the antibody INRA-RU1 (Ralet et al. 2010), which recognizes at least six repetitions of the disaccharide rhamnose-galacturonic acid. The collected data show the presence of the epitope in the middle lamella of bast fibers (Fig. 3a–c). At H9, the INRA-RU1 signal is indeed mainly detected in the middle lamella delimiting the bast fibers (Fig. 3a, arrowheads). The signal is also prevalent in the middle lamella at H15 (Fig. 3b, arrowhead), a stage where the development of the G-layer is quite evident. Conversely, at H20, the INRA-RU1 signal is intense in the
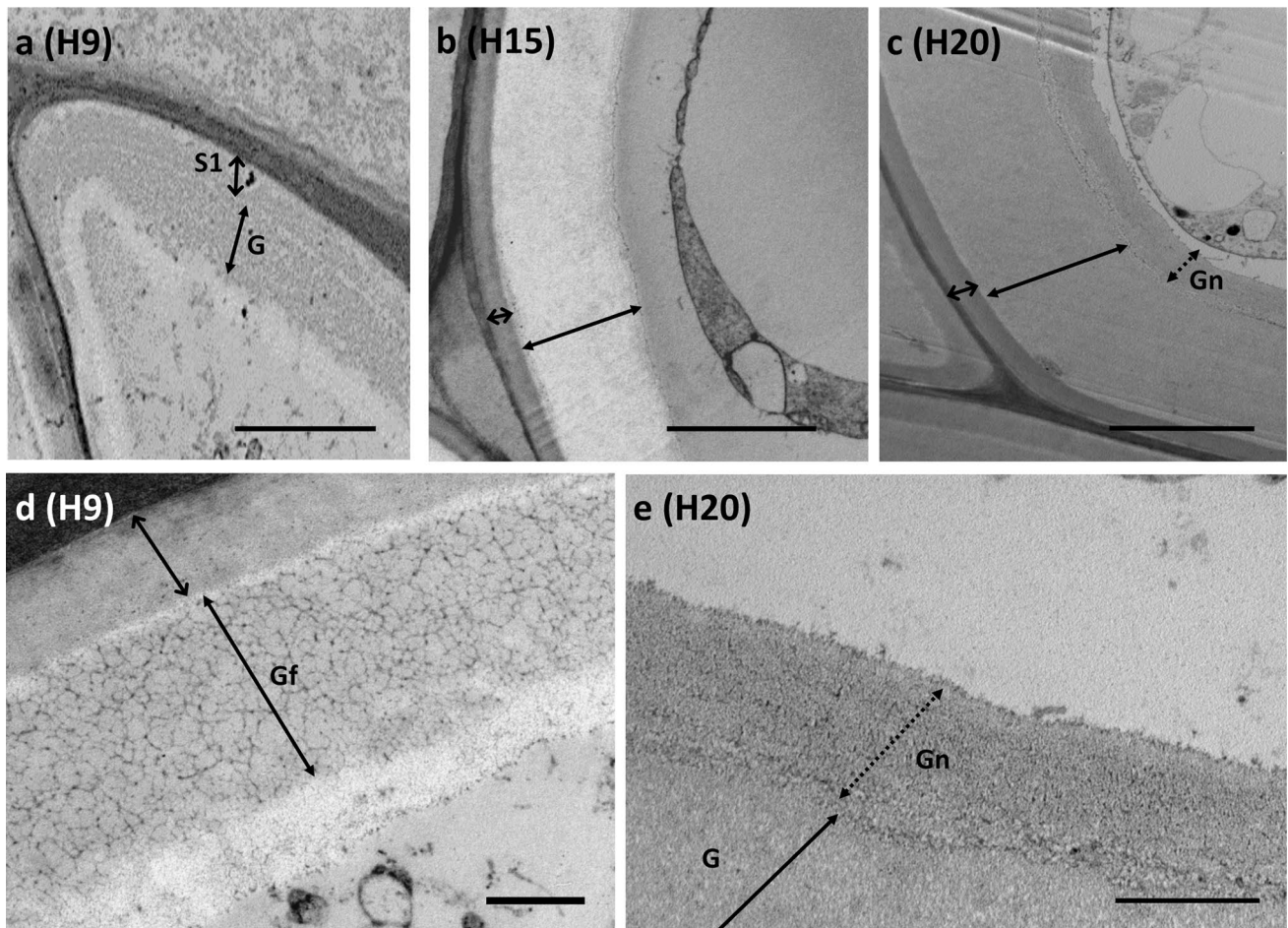
Fig. 1 Ultrastructural analysis of bast fibers in hemp stems at different developmental stages. **a** After 9 days of growth (H9), bast fiber cells already highlight the presence of secondary cell wall and it is possible to distinguish a first layer (S1, double arrow) and the initial gelatinous layer (G-layer, indicated by the double full arrow). **b** Bast fibers at the stage of development H15, where the increase in thickness of the G-layer is clear. **c** At the developmental stage H20, the increase in thickness of the G-layer (double full arrow) is most noticeable. At this stage, it is possible to notice the presence of an additional fibrillar layer, which presumably corresponds to the Gn-layer. Bars **a**–**c**: 2 μm. **d** Early stage of development in which the G-layer is characterized by a messy intertwined array of fibrils (which is defined as "Gf layer"). **e** Detail of a more compact G-layer and of the fibrillar layer Gn, in which it is possible to recognize its cellulosic nature. Bars in **d**, **e**: 500 nm

middle lamella and, perhaps, also in the PCW of bast fibers (Fig. 3c). However, the G-layer of bast fibers is labelled too, showing that at this developmental stage the presence of RG-I is a consistent trait of the gelatinous cell wall (Fig. 3c).

Arabinans are important components of pectic polysaccharides, namely RG-I. They also decorate arabinogalactan proteins (AGPs) (Mollard and Joseleau 1994). In this work, we have determined their localization using the antibody LM6 directed against (1-5)-α-ʟ-arabinan (Willats et al. 1998). At H9, the distribution of arabinans depends on the cell type analyzed. In parenchyma cells, arabinans are observed in the middle lamella (Fig. 4a, arrowhead); in this case, no distinctive pattern is observed. On the contrary, in developing bast fibers, the distribution of arabinans is slightly different, because the antibody signal is detected at the interface between the cytoplasm and the G-layer (Fig. 4b, arrowhead), with the signal being very poor within the developing SCW (square bracket). This indicates a process of deposition or secretion of arabinans, while the gelatinous cell wall is assembled, or labelling of proteins decorated with arabinans (see "Discussion") and located at the interface between the membrane and the cell wall. In H15, the distribution of arabinans is different because they are virtually absent in the PCW and are quite dispersed in both the S1- and the G-layer; in both cases, the signal is relatively weak, and no appreciable differences are detectable between the two cell wall layers (Fig. 4c). This type of distribution does not change radically in H20, where the signal intensity is still relatively low; nevertheless, a stronger accumulation of gold particles is observed in the S1-layer (Fig. 4d, e). In
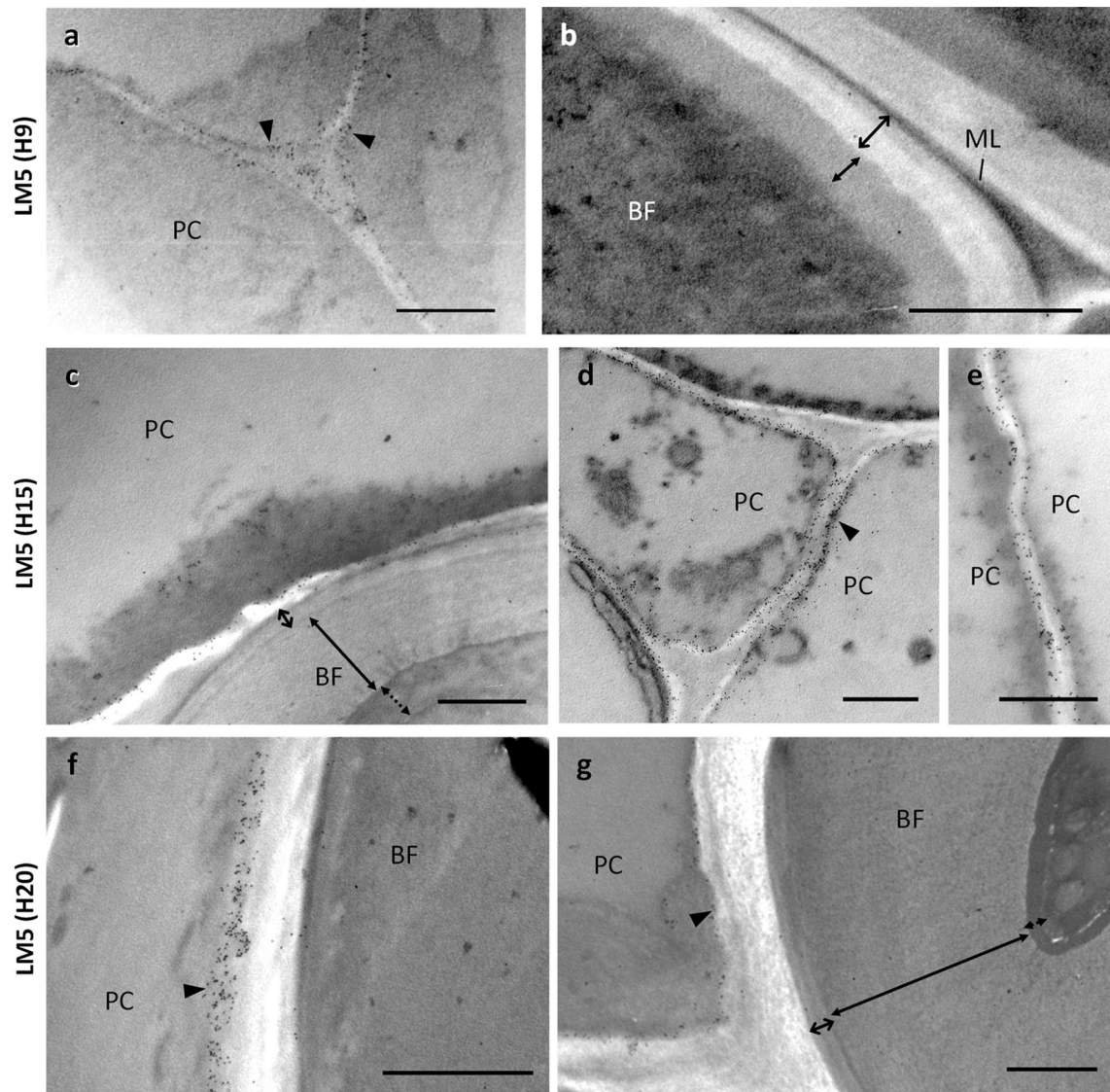
Fig. 2 Galactan distribution assayed with the LM5 antibody. **a** At H9, the signal is found in the cell walls of parenchyma cells (PC) (arrowheads) Bar: 1000 nm. **b** In the bast fibers (BF), the signal is very weak or absent. *ML* middle lamella. Bar: 1000 nm. **c** At H15, the galactan distribution does not change with the parenchyma cell wall still uniformly labelled, while the cell wall of bast fibers does not show any labelling. Bar: 1000 nm. **d–e** Cells of the parenchyma in which the LM5 signal is strong and limited to the cell wall (arrowhead). Bars: 1000 nm. **f** The immunolabelling signal is distinct in the cell wall of parenchyma cells (arrowhead) but absent in the cell walls of bast fibers. Bar: 1000 nm. **g** A typical bast fiber with a thickened cell wall in which the LM5 signal is absent in both the G- and the S1-layer. In contrast, the adjacent parenchyma cell shows a constant signal but limited to the cell wall (arrowhead). Bar: 1000 nm

the G-layer, the density of gold particles is extremely low; it is nevertheless noteworthy that a certain amount of signal is observable in the developing G-layer (Fig. 4d, arrowhead).

Distribution of xylan

Xylans are critical components of the SCW, where they contribute to the overall plant defense against herbivores and pathogens and to the recalcitrance of lignocellulosics (Rennie and Scheller 2014). The distribution of xylans was investigated using the LM10 antibody, which specifically recognizes both unsubstituted and relatively low-substituted xylans in different species (McCartney et al. 2005) or, alternatively, the nonreducing ends of xylans (Ruprecht et al. 2017). The distribution pattern of xylans changes during the development of bast fibers, from H9 to H20. In H9 (Fig. 5a, b), xylans are very abundant both in the cell walls of developing xylem cells (Fig. 5a) and in the cell walls of bast fibers (Fig. 5b). In this case, the signal is comparably distributed both in the S1- and G-layers. At H15, the signal distribution changes significantly. While many gold particles are clearly observable in the S1-layer,
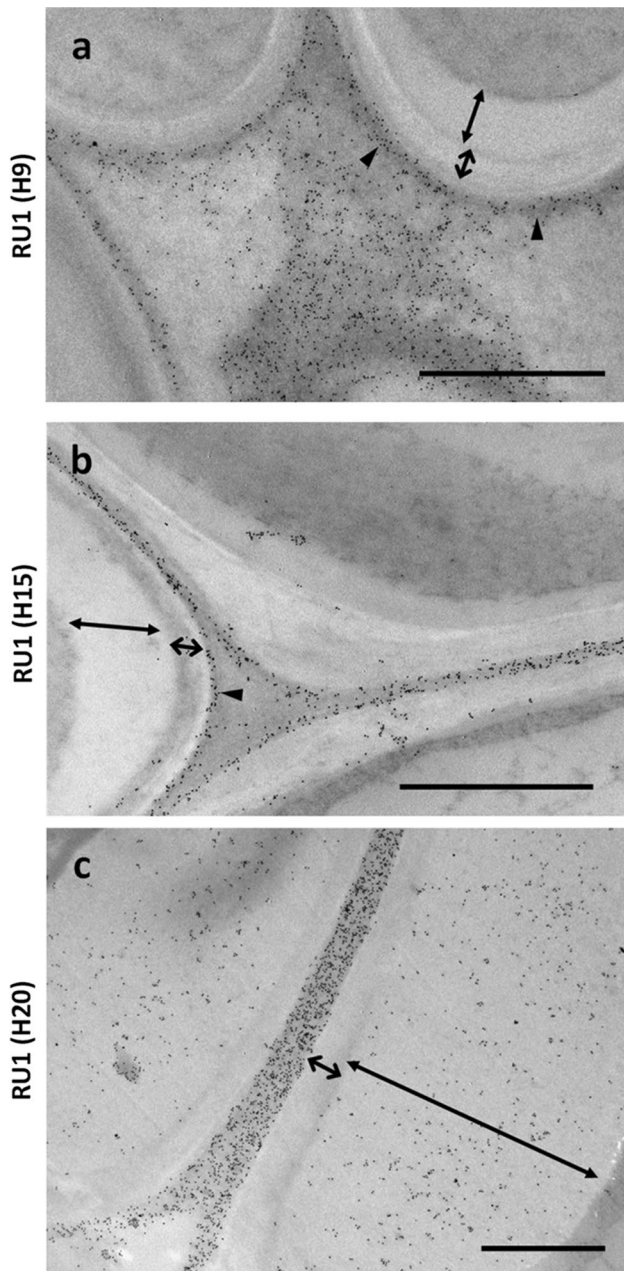
Fig. 3 Rhamnogalacturonan I distribution assayed with the INRA-RU1 antibody. **a** At H9, the signal in present in the middle lamella delimiting the bast fibers. **b** At H15 the development of the G-layer is evident, and the signal is prevalent in the middle lamella. **c** At H20 the signal is intense in the middle lamella and in the PCW of bast fibers. A signal is also present in the G-layer of bast fibers. Bars: 1000 nm

they are absent in the G-layer (Fig. 5c, d). This agrees with what was recently shown in hemp using the LM11 antibody (Chernova et al. 2018). The distribution pattern is preserved and reinforced in sections of bast fibers at H20 (Fig. 5e, f). Here, the signal is significantly stronger in the S1-layer but is absent both in the G-layer and in the

PCW. The densitometric analysis shows the presence of a substantial xylan signal at the level of the S1-layer and the simultaneous absence of signal in the G-layer at any developmental stage (Fig. S4a). The partial signal of xylans at H9 in the region corresponding to the developing G-layer could represent a residue of xylans deposited in the neighboring S1-layer, but not necessary for the development of the G-layer. The data at H15 and H20 clearly indicate that xylans are critical for the correct assembly of the S1-layer, but not of the G-layer.

Distribution of crystalline cellulose

We analyzed the distribution of crystalline cellulose using the CBM3a probe (which binds the hydrophobic surface of crystalline cellulose). Cellulose is the main load-bearing polysaccharide of cell walls and its distribution helps determining the level of mechanical resistance. In bast fibers at H9, the signal of crystalline cellulose is in two distinct regions, respectively, in the S1 layer and as a crystallization front in the G-layer originating from the area nearest the plasma membrane and then propagating to the residual G-layer during the H15 and H20 stages (Fig. 6a, b). The signal in the S1-layer (approx. 200–250 nm) is higher than the signal in the G-layer region closest to the plasma membrane (approx. 150 nm). The two regions with higher intensity are interspersed with a cell wall space representing the assembled G-layer that has lower crystalline cellulose signal. The PCW appears devoid of signal. At H15, the pattern of crystalline cellulose changes drastically. The S1-layer is characterized by a higher signal, as shown by a high density of gold particles, while the whole G-layer contains, in comparison, a much lower signal (Fig. 6c, d).

The densitometric analysis on images after thresholding (Fig. S4b) reveals that the S1-layer is characterized by a signal of crystalline cellulose up to 10 times higher than that present in the G-layer. The signal in the S1-layer is distributed for a thickness of about 250 nm. At H20, the situation previously described in H15 is maintained, even if the signal density seems to decrease generally (Fig. 6e, f). The signal is absent in the PCW, it is relatively high in the S1-layer and then becomes very weak in the G-layer, as also confirmed by densitometric analysis. The quantification of the signal after thresholding (Fig. S4b) shows that crystalline cellulose is absent in the PCW, it constantly accumulates in the S1-layer of the SCW independently from the developmental stage, but is conversely distributed in the G-layer according to the specific phase of development of this cell wall layer. Crystalline cellulose is abundant in the G-layer at H9, but decreases at H15, as well as at H20. This suggests that crystalline cellulose has distinct roles between the S1 and G-layers.

Fig. 4 Analysis of the distribution of arabinans with the LM6 antibody. **a** At H9, arabinans vary in distribution depending on the cell analyzed. In the parenchyma, arabinans are observed in the middle lamella (arrowhead). **b** At the level of developing bast fibers, arabinans localize mainly at the interface between the cytoplasm and the gelatinous cell wall (arrowhead), with a weak signal in the G-layer (square bracket). Bars: 1000 nm. **c** At H15, arabinans are absent in the PCW and faintly dispersed in both the S1- and G-layers. Bars: 500 nm. **d**, **e** The distribution does not change at H20, with the signal still weak, but also showing accumulation in the S1-layer. In the G-layer, the signal intensity is weak, but a certain amount of signal (arrowhead) is observable in the inner interface, presumably the Gn-layer (dotted double arrow). Bars: 500 nm
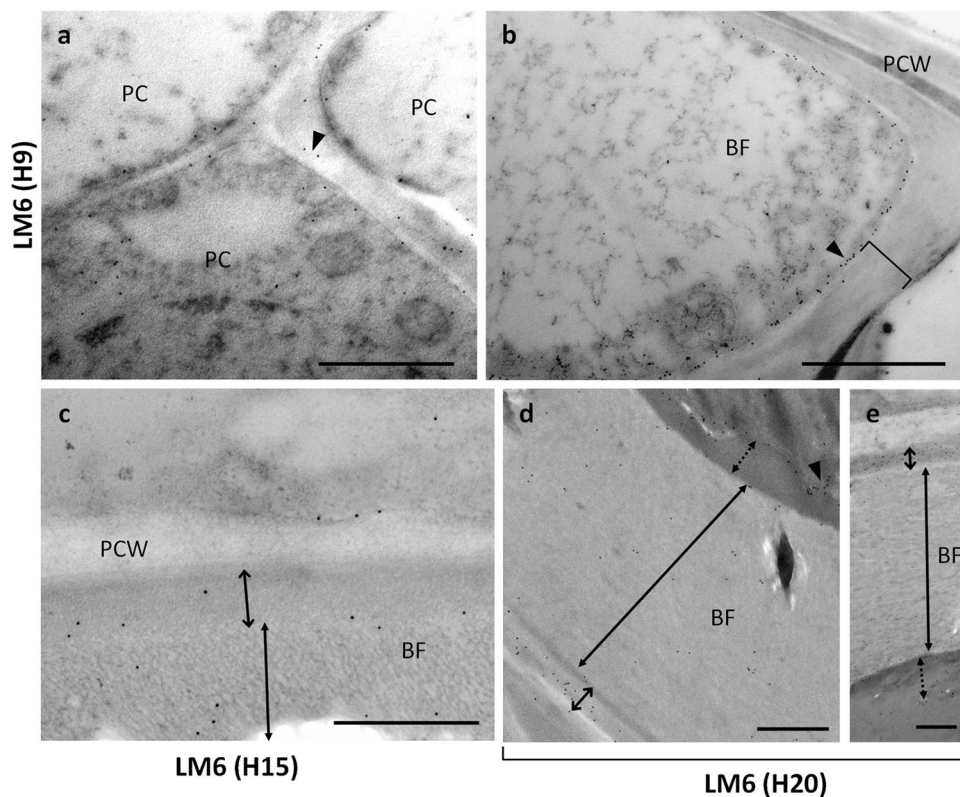
## Distribution of a class III peroxidase and a laccase

The specificity of CsaPRX64 was checked by Western blotting on an extract of hemp cell wall proteins obtained from the woody core (Fig. 7a). A major signal was detected at the expected size of the protein (ca. 34 kD). To confirm the antigen, the proteins present in the extract were separated with a 2D-gel and identified by MALDI-MS/MS (Fig. 7b). Most proteins identified are class III peroxidases (CsaPRX3 and CsaPRX52). This result confirms the suitability of this Ab to study the localization of class III peroxidases in hemp. Class III peroxidases are important enzymes for the lignification of fibers (Novo-Uzal et al. 2013). CsaPRX64 was specifically observed because its coding gene was significantly more expressed in H20 as compared to H9 (129 vs 552 RPKM; Behr et al. 2016).

The resulting signal with the CsaPRX64 antibody is relatively widespread at H9. During the development of bast fibers, the signal is found in the cell cytoplasm (arrowheads in Fig. 8a), while a weak one or no signal at all is detected in the cell walls. However, the peroxidase distribution is different in parenchyma cells (Fig. 8b), because in this case a considerable number of gold particles is visible inside the cell walls (arrow). The insert in Fig. 8b shows a developing bast fiber with the nucleus. In H15, the signal density is significantly higher than the one observed in H9. Both the S1- and the G-layer show an uneven distribution of gold particles.

The signal is weaker in the S1-layer but increases in the direction of the developing G-layer (Fig. 8c, d). This type of distribution is also essentially preserved in H20, although with some modifications, mainly because the density of gold particles in the G-layer is more homogeneous. The S1-layer also showed a lower signal intensity (Fig. 8e, f). As a result, it seems that the peroxidase(s) detected by the hemp PRX64 antibody initially accumulate(s) in the cytoplasm and are then secreted into the cell wall during the development of the secondary layers; their role seems to be particularly important in the development of the G-layer, but it is less critical for the development of the S1-layer.

Laccases are critical enzymes in the assembly of the SCW because they are oxidative enzymes that determine the lignification of cell wall. First, we analyzed the specificity of the antibody by dot blot assay against the purified immunogenic peptide and then against protein extracts from hemp stems and leaves (Fig. 9). As can be seen, the signal intensity is higher in the proteins extracted from the stem, a tissue that contains more lignified tissues, as compared to leaves. The distribution of laccase recognized by the CsaLAC17 antibody was then investigated during the development of bast fibers. We studied the distribution of this laccase because its coding gene is significantly expressed in H20, as compared to H9 (62 vs 163 RPKM) (Behr et al. 2016). In H9, the enzyme shows a relatively homogeneous distribution in the developing bast fibers and the antibody signal can be

Fig. 5 Distribution of xylans as highlighted with the LM10 antibody. **a**, **b** At the H9 stage, xylans are abundant both in the cell walls of xylem and in the cell walls of bast fibers; in the latter, the level is comparable between S1- and G-layers. Bars: 1000 nm. **c**, **d** At H15, the signal is clearly observable in the S1-layer but is absent in the G-layer. Bar in **c**: 1000 nm; bar in **d**: 500 nm. **e**, **f** Similar data are evident at H20, where the signal is stronger in the S1-layer but is absent both in the G-layer and in the PCW. Bars: 1000 nm
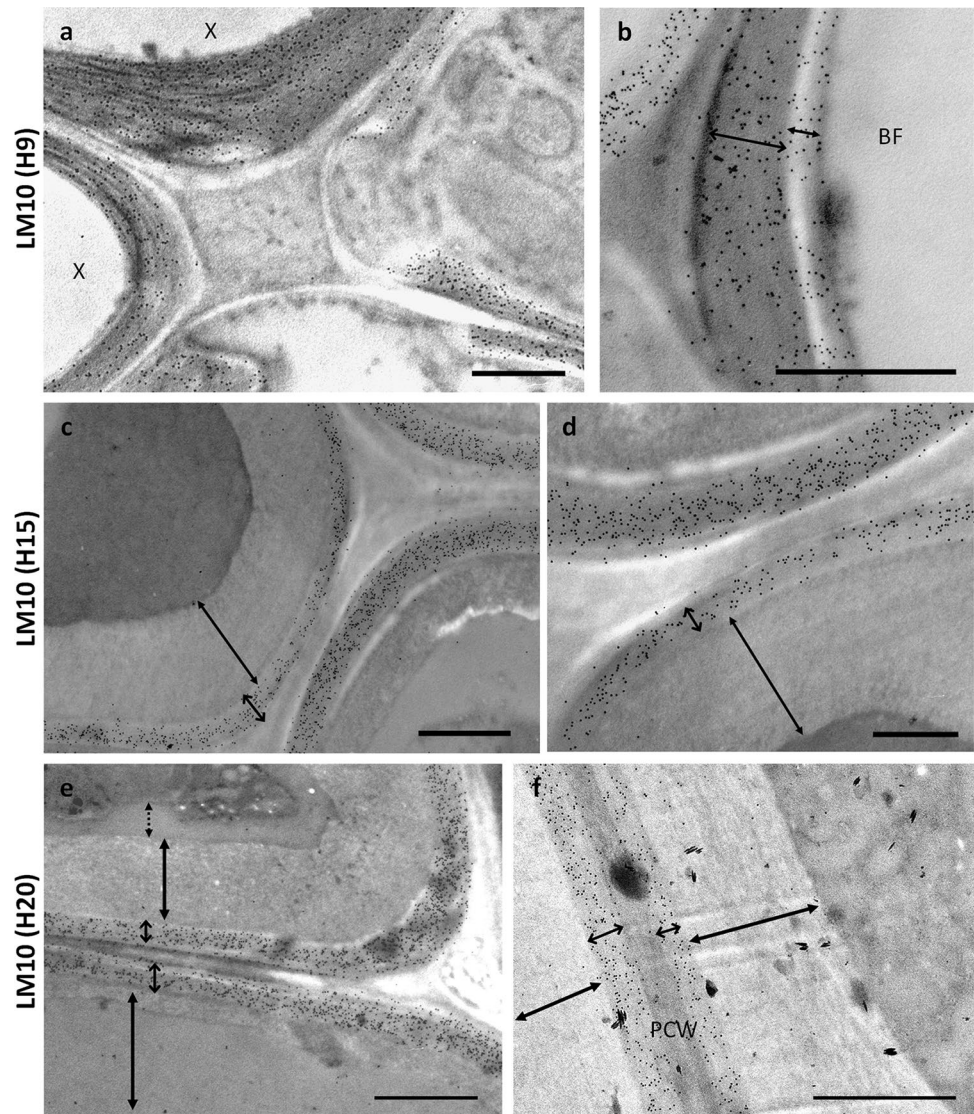
observed both in the developing cell wall, as well as inside the cytoplasm (Fig. 10a, arrowheads). Due to low signal intensity, no statistical analysis was performed. On the contrary, the distribution pattern is different in H15. In this case, most of the signal distinctly accumulates at the interface between the S1- and the G-layer (Fig. 10b). The laccase signal is absent in the S1-layer, but it is distinctly found in the first 100 nm of the G-layer in contact with the S1-layer. No signal is found in the PCW. At H20 the laccase distribution is partially different, with a substantial accumulation of epitopes in the whole thickness of the G-layer and the density of gold particles is homogeneous (Fig. 10c). Even at this developmental stage, no consistent signal is observed in PCW and not even in the underlying S1-layer of the SCW (Fig. 10d). The densitometric analysis (Fig. S4c) confirms that the laccase is not present (or poorly present) in the PCW and in the S1-layer of the SCW at H15. On the contrary, the G-layer is strongly labelled in the half facing the S1-layer,

then the signal becomes progressively weaker. This labelling pattern is maintained in H20, although the signal extends throughout the thickness of the G-layer; a faint signal is also observed in the S1-layer, but it can be interpreted as background.

Discussion

In this manuscript, we provide information on the ultrastructural changes accompanying the development of the hemp hypocotyl. Additionally, we analyze the distribution of major cell wall polysaccharide classes (cellulose, xylan, pectic polysaccharides) and provide additional novel data relative to the distribution of a hemp peroxidase and a laccase. We validate the hemp hypocotyl to address cell wall-related studies during elongation and thickening: our transcriptomic analysis indeed confirms the upregulation of xylan and SCW

Fig. 6 Distribution of crystalline cellulose with the CBM3a probe. **a**, **b** In bast fibers at H9 stage, crystalline cellulose is found at the assembly points of layers S1 and G. The primary cell wall (PCW) is signal-free. Bars: 1000 nm. **c**, **d** At H15, the distribution of crystalline cellulose changes drastically because the S1-layer has a stronger signal while the G-layer has a weak signal. Bars: 1000 nm. **e**, **f** In H20, the situation is similar to that described for H15 although the signal strength decreases. The signal is absent in the PCW, relatively intense in the S1-layer and weaker in the G-layer. Bar in **e**: 500 nm; bar in **f**: 200 nm
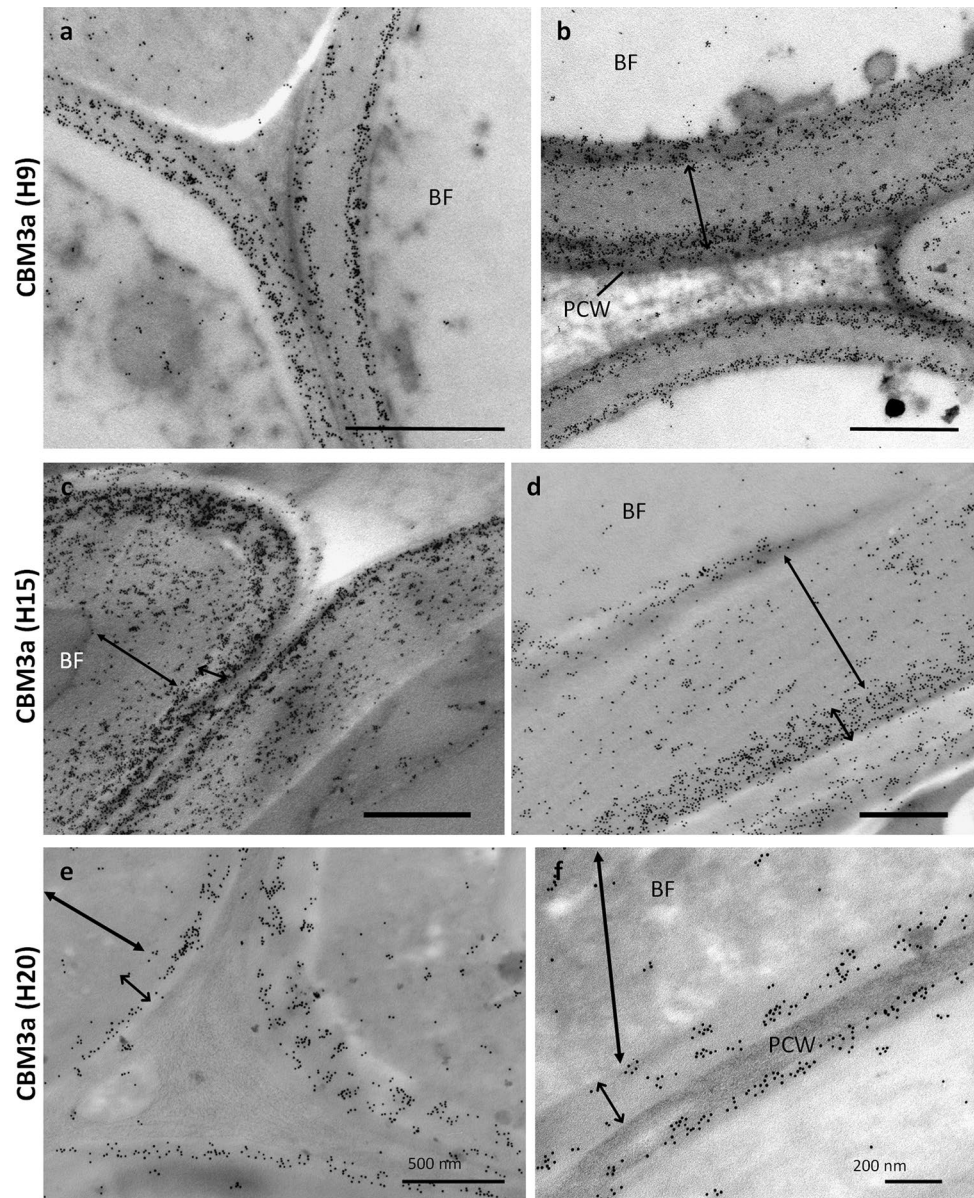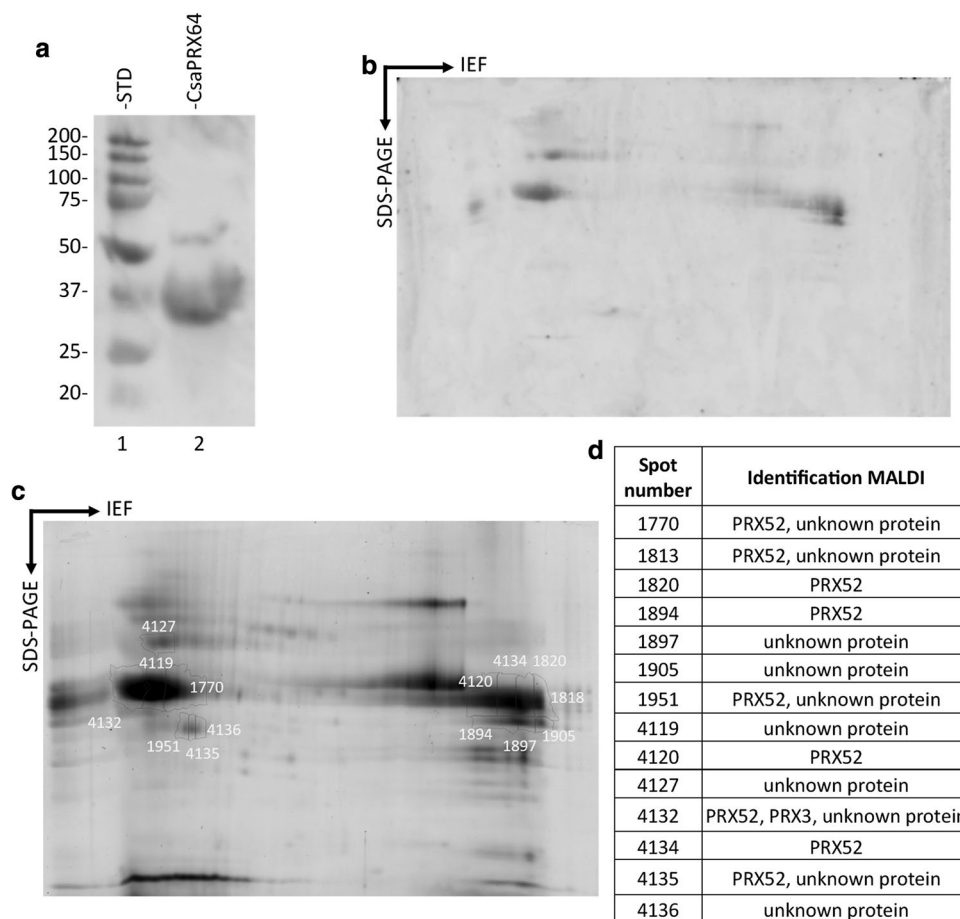
cellulose biosynthetic genes during development (Fig. S2 and S3). More specifically, we show the upregulation of genes involved in xylan backbone elongation (such as *GUT1* and *GUT2*) in H15 and H20, as well as of *GUX2* and *GUX4* (substitution of xylan with glucuronic acid), *GXM3* (catalyzing 4-*O*-methylation of glucuronic acid) and *ESK1* and *RWA3* (xylan acetylation). It will be of biological interest to study, separately, the expression of those genes in the xylem (xylan-type cell wall) and in the bast fibers (which are characterized by a gelatinous cell wall). The chemical composition of xylan in these two tissues may be regulated to fulfil distinct functions, such as water conduction in xylem vessels and mechanical resistance in phloem fibers. Genes involved in cellulose biosynthesis (*CesA4*, *CesA7* and *CesA8*) and crystallization (*COBRA*, *COBRA-LIKE4*) were upregulated

in H15 and H20, stages coinciding with thickening of bast fiber cell walls. Similar to what was reported in phloem fibers from older internodes of adult stems (Guerriero et al. 2017), the expression of some *FLA*s is induced during the girth increase of the hypocotyl, a finding further corroborating the validity of the hemp hypocotyl as a model for bast fiber cell wall studies.

Ultrastructural changes in the bast fibers during the development of the hemp hypocotyl

The ultrastructural details revealed with electron microscopy make it possible to distinguish the specific cell wall layers of bast fibers. Several interesting features have been unveiled in our study. First, at young developmental stages (H9), the

Fig. 7 Characterization of the antibody to peroxidase. **a** Western blot characterization of CsaPRX64 on an extract of hemp cell wall proteins prepared according to Printz et al. (2015). The signal appears at the expected size (34 kD). Lane 1, standard of molecular weight in kD; lane 2, western blot with CsaPRX64. **b** Complementary characterization of CsaPRX64 by 2D-Western blot. **c** Corresponding 2-D gel used for MALDI analysis. **d** MALDI-MS/MS identification; CsaPRX64 hybridizes with CsaPRX3 and CsaPRX52, two peroxidases involved in lignification

Spot number	Identification MALDI
1770	PRX52, unknown protein
1813	PRX52, unknown protein
1820	PRX52
1894	PRX52
1897	unknown protein
1905	unknown protein
1951	PRX52, unknown protein
4119	unknown protein
4120	PRX52
4127	unknown protein
4132	PRX52, PRX3, unknown protein
4134	PRX52
4135	PRX52, unknown protein
4136	unknown protein

S1-layer of bast fibers is electron-lucent (Fig. 1a), a feature highlighting structural differences with that found at older stages, where the S1-layer is instead electron-dense (Fig. 1b, c). Such a feature could be due to the deposition of lignin (Reza et al. 2015), which, despite being a minor component in bast fibers, is deposited for mechanical reasons as the hypocotyl ages. Additionally, we here report the presence of a transient stage in the assembly of the G-layer (which we name Gf) (Fig. 1d). Such a "loose" cell wall is observed in the young hypocotyl (H9) and is transitory because it is not observed at H15/H20. We propose that such a transient stage precedes the maturation of the compact and more homogeneous crystalline G-layer and is due to loosely-bound cellulose fibers. The previously reported "stripped" Gn-layer in adult hemp (Chernova et al. 2018) is here observed at H20 (Fig. 1c, e) and found to be smaller in width than the crystalline G-layer (Fig. 1c).

Characterization of the non-cellulosic matrix polysaccharides in the bast fibers of the hemp hypocotyl

Gelatinous cell walls are characterized by cellulose microfibrils parallel to the longitudinal cell axis, as well as NCPs, such as RG-I, which are crucial for their biomechanical properties (Goudenhooft et al. 2018). In several species, such as flax, NCPs display high percentages of galactose-containing polymers. Hypothetically, the secretion of soluble galactans plays a role in the axial orientation of the cellulose microfibrils, while the subsequent cross-linking of galactans could be related to the assembly of the S2-layer (Gorshkova and Morvan 2006). Although these data suggest the importance of galactans during the assembly of the SCW, their precise abundance and distribution is still debated, as well as their relative distribution. In flax bast fibers, the main non-cellulosic component of the gelatinous cell walls is galactan, which is part of RG-I closely associated with cellulose. In this plant, the formation of the gelatinous cell wall is accompanied by the accumulation of Golgi vesicles that fuse with the plasma membrane. Both Golgi vesicles and cell wall layers are labelled by LM5 antibody, thus indicating the presence of (1,4)-β-galactan (Salnikov et al. 2008). Numerous studies carried out in flax suggest that, during fiber development, a matrix enriched with galactan (Gn-layer) is gradually modified into the G-layer, rich in cellulose (Gorshkova et al. 2004; Gorshkova and Morvan 2006; Chernova et al. 2007; Gur'janov et al. 2007; Salnikov et al. 2008; Roach et al. 2011). This process is dependent on the

Fig. 8 Analysis of peroxidase distribution. **a** The signal is diffused at the H9 developmental stage of bast fibers and is mainly localized in the cytoplasm (arrowheads). **b** Peroxidase distribution is different in parenchymatic cells because an intense signal is visible inside the cell walls (arrow). Inset in **b**: a developing bast fiber. Bars in **a** and **b**: 1000 nm. **c, d** In H15, the signal density is higher than in H9 and both the S1 and G-layers show an irregular signal that increases in the direction of the developing G-layer. Bars in **c** and **d**: 1000 nm. **e, f** The distribution is maintained in the H20 stage where the signal density in the G-layer is more homogeneous and the S1 layer shows a lower intensity. Bars in **e** and **f**: 1000 nm
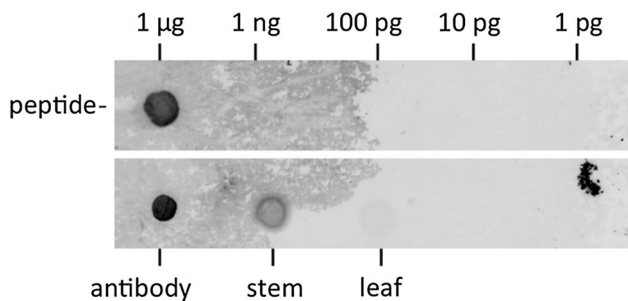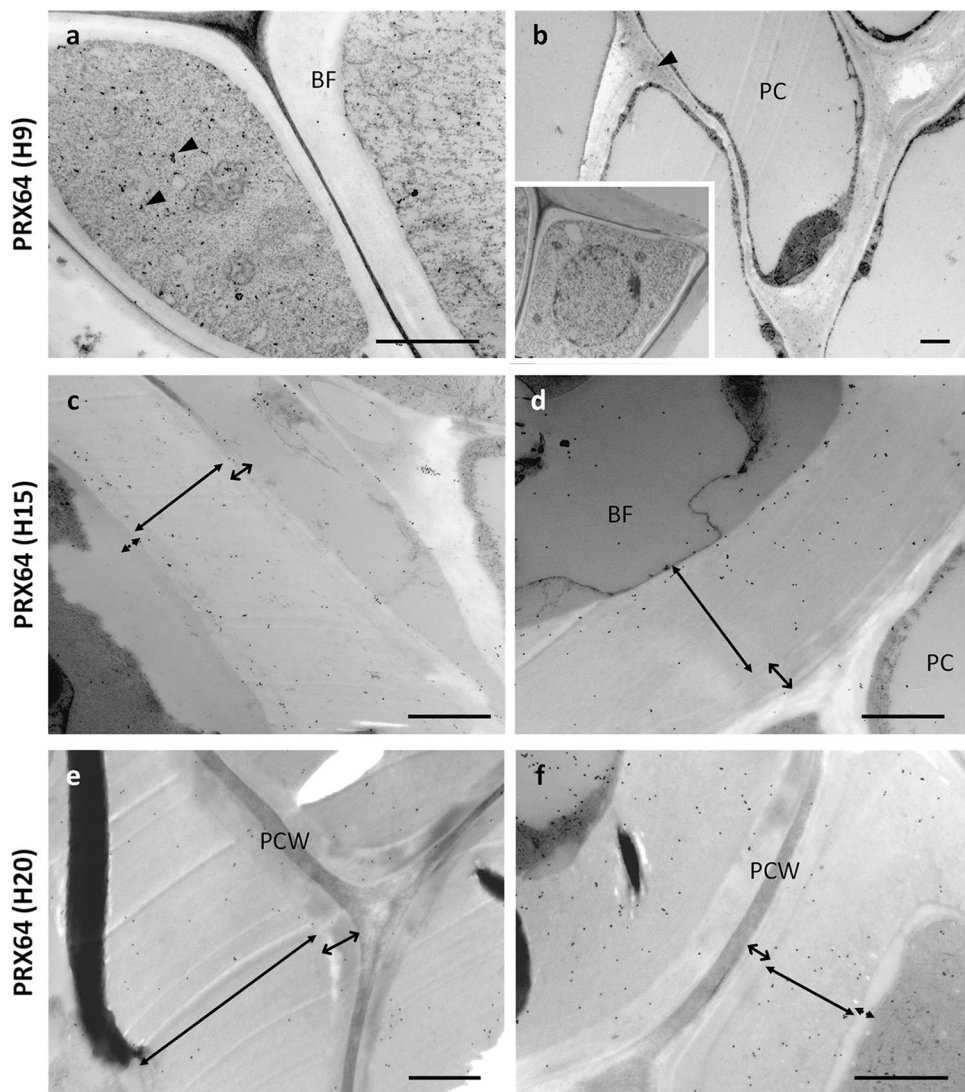

Fig. 9 Dot blot assay of anti-laccase antibody. The antibody was tested against the purified antigenic peptide (first row), spotted in serial dilution. The second row reports the control of the detection between antibodies and the assay of the anti-laccase antibody on crude protein extracts from stems and leaves of hemp. The protein loads are as follows: 2.7 μg of stem proteins, 3 μg of leaf proteins

expression of a β-galactosidase. Consequently, transgenic flax with reduced activity of β-galactosidase shows lower concentrations of free galactans and, therefore, a significant reduction in the thickness of the cellulosic G-layer. In contrast, the Gn-layer, as labelled by the LM5 antibody, is significantly expanded (Roach et al. 2011). The expression and activity of β-galactosidase is therefore necessary for the dynamic remodeling of polysaccharides in flax bast fibers (Roach et al. 2011).

Studies carried out in hemp have emphasized that (1-4)-β-D-galactans recognized by LM5 are not present in the G-layer (Blake et al. 2008; Behr et al. 2016; Chernova et al. 2018) and our observations (Fig. 2) confirm this from an immuno-ultrastructural point of view. β-Galactans, as identified by LM5, are in the cell walls of parenchyma cells but not in those of bast fibers and this for each of the analyzed developmental stages. A weak detection with LM5 was obtained only when the polysaccharide fraction

Fig. 10 Distribution of laccase. **a** The signal is widespread in H9, with no preference for distribution (arrowheads). Bar: 1000 nm. **b** In H15, there is significant accumulation of signal at the boundary between the S1 and G-layers; the signal is absent in the PCW and in the S1-layer. Bar: 1000 nm. **c, d** In H20, the signal is observable throughout the thickness of the G-layer but is absent in the S1-layer. Bars: 1000 nm
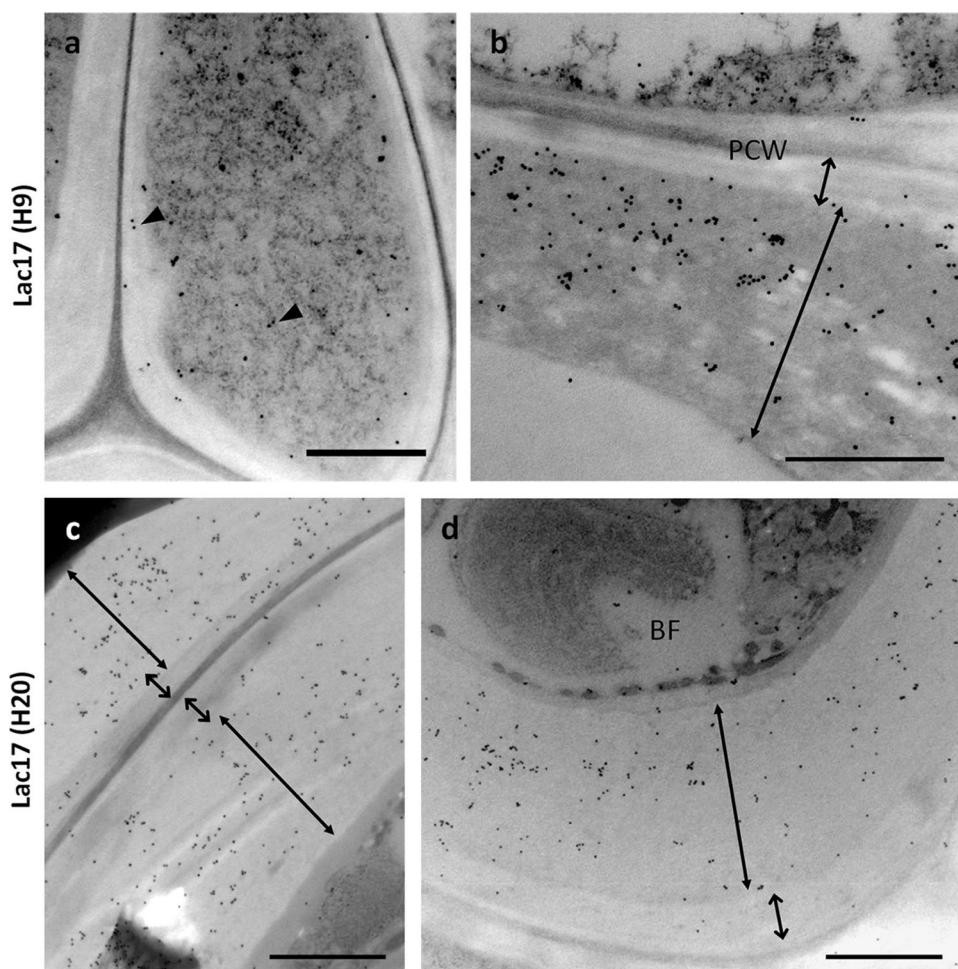
was isolated from hemp bast fibers (Chernova et al. 2018). Although this weak signal may lead to the hypothesis of a "masking" effect in the cell wall, it is also plausible that the content of galactans with relatively long $1\rightarrow4$-β-galactosyl residues is very low and they are consequently not detected.

To provide information about the structure of hemp RG-I, the INRA-RU1 Ab is used (Fig. 3). This antibody best recognizes the motif R7-U7 (seven repeats rhamnose-galacturonic acid) and shows activity towards R6U6, R8U8, and R9U9 (Ralet et al. 2010). In H9 and H15, the signal is confined to the pectinaceous middle lamella, while in H20 labelling of the G-layer is clear. We did not have sections for immunodetection with INRA-RU1 displaying the "stripped" layer in H20 (Fig. 1c, e), which showed binding to INRA-RU2 (Chernova et al. 2018); however, our results confirm the presence of RG-I in the G-layer. The RG-I found in the middle lamella functions as a sort of adhesive between neighboring cells, while it contributes to the creation of tension in the G-layer through lateral interaction with cellulose microfibrils (Mikshina et al. 2015). The composition of RG-I from the middle lamella is relatively stable between species, as opposed to the RG-I present in the G-layer.

Arabinans are components of RG-I, as well as AGPs (Mollard and Joseleau 1994) and are involved in several functions. In cotton, the middle lamella is fundamental for cellular adhesion and separation during fiber development. The structural and compositional analysis of the middle lamella reveals that it is composed of various sugars, such as homogalacturonan, xyloglucan, and arabinan. While xyloglucan is abundant in bulges of the cell wall, arabinans are absent in these regions (Hernandez-Gomez et al. 2017). Modifications in arabinan levels were also observed during floral abscission, as a strong increase of xyloglucan, galactan, and arabinan was observed during fruit development in tomato (Iwai et al. 2013). Therefore, it seems that the relative percentage of arabinans can affect the structural properties of the cell wall. This heterogeneity of function is also reflected in the distribution of arabinans during the development of the gelatinous cell wall in hemp, as detected by the LM6 antibody. First, we observe discrepancies in the signal between parenchyma cells and bast fibers (Fig. 4). Second, the pattern of arabinan deposition during the development of the G-layer follows a scheme that is not easy to interpret. In this respect, it should be noted that this Ab

shows binding to some arabinogalactan proteins (AGPs) too (Lee et al. 2005; El-Tantawy et al. 2013), therefore the signal detected in the hemp sections can also be indicative of the presence of these glycosylated proteins. In the hemp hypocotyl, arabinans are initially observed at the interface between the cytoplasm and the G-layer; subsequently they accumulate in the developing secondary wall but, at H20, they are almost exclusively present in the S1-layer. It seems therefore possible to hypothesize that arabinans are necessary for the process of SCW assembly in bast fibers, but only in relation to the S1-layer.

Xylan and cellulose distribution in hemp hypocotyls

Xylan is the principal hemicellulose in SCW of vascular and sclerenchyma supporting tissues. The monoclonal antibodies LM10 and LM11 (usually used to detect xylans) have different specificity: LM10 is specific for unsubstituted or low-substituted xylans, while LM11 binds to low-substituted xylans, as well as arabinoxylans (McCartney et al. 2005). Recently, LM11 was shown to label the S1-layer of hemp bast fibers (Chernova et al. 2018).

In hemp hypocotyls, labelling with LM10 shows a strong signal in the xylem cells (Fig. 5) and, as shown for LM11, in the S1-layer of the SCW of bast fibers. The G-layer, instead, is devoid of LM10 signal (Fig. 5). The stronger signal with respect to the recently reported LM11 (Chernova et al. 2018) indicates the presence of unsubstituted/low-substituted xylans in the hemp S1-layer.

In our analysis of hemp bast fibers, we found that crystalline cellulose is localized in the S1-layer of the SCW, while the signal is less abundant in the G-layer (Fig. 6). This feature has already been observed in bast fibers of flax hypocotyl, where affinity labelling of crystalline region of cellulose evidenced a higher signal in the half of the SCW closest to the PCW (Andeme-Onzighi et al. 2005). This differential distribution distinguishes the two cell wall layers. In some ways, this feature is different from what is found in the tension wood of trees, where it represents one of the straightening mechanisms allowing trees to resume erected growth. Tension wood is characterized by a G-layer enriched in crystalline cellulose near the lumen of tension wood fibers (Bhandari et al. 2006). It is important to note here that CBM3a shows binding to xyloglucan too (Hernandez-Gomez et al. 2015). Earlier analyses using the xyloglucan-specific Ab LM15 and confocal microscopy revealed that in the young hemp hypocotyl a strong signal was only detected in the developing xylem (Behr et al. 2016). The signal became detectable in primary bast fibers only in H15 and it subsequently decreased in H20 to become homogeneous across the entire hypocotyl section. Therefore, we cannot rule out the possible contribution of xyloglucan to the signal observed, at least in H15 (Fig. 6c, d). As previously

discussed in the literature, a treatment with xyloglucanase can provide detailed information of crystalline cellulose distribution in plant cross sections (Hernandez-Gomez et al. 2015).

G-layers are characterized as highly abundant in crystalline cellulose (Roach et al. 2011; Mellerowicz and Gorshkova 2012); one reason for the observed overall low CBM3a signal could be due to the accessibility of crystalline cellulose in function of variations in microfibril angle (MFA) at the nanoscale level, or in relation to masking by NCPs (Ruel et al. 2012).

Localization of cell wall proteins in hemp hypocotyls

Peroxidases are enzymes involved in the lignification process, even if not only in SCWs. For example, in cell cultures of *Populus tremula*, cells produce PCW that are lignified. Cells show peroxidase activities, which increase during lignin formation (Christiernin et al. 2005). Such enzymatic activities are usually associated with the production of hydrogen peroxide. In *Zinnia elegans* L. (one of the most useful models for the study of tracheary element differentiation), lignification is characterized by a high production of ROS (hydrogen peroxide), necessary for the polymerization of monolignols. The role of ROS in regulating different cell wall-related processes, like extension and lignification, is known (Berni et al. 2019).

Hydrogen peroxide indeed acts as a signaling molecule in the regulation of fiber elongation. In cotton, the *GhAPX1AT* gene codes for an ascorbate peroxidase. Plants with down-regulation of *GhAPX1AT* are characterized by a significant increase in the number of fibers and by oxidative stress, which significantly reduces fiber elongation. During gene overexpression, cells show enhanced tolerance to oxidative stress suggesting that optimal levels of hydrogen peroxide are key mechanisms regulating fiber elongation (Guo et al. 2016).

Our results show that the peroxidase detected by the CsaPRX64 antibody has a distribution not exactly correlated with the lignification process of the S1-layer (Fig. 8). Indeed, most of the signal is in the G-layer, with a scarcity or absence of signal in the S1-layer. If the S1-layer is lignified, the peroxidase detected by CsaPRX64 antibody is most likely involved in other processes of modification of the gelatinous cell wall, or in cellular defense mechanisms. Several class III peroxidases, such as AtPRX34 and AtPRX57, are involved in cell wall loosening through breaking covalent bonds within cell wall polymers (Francoz et al. 2015). Upon production of reactive oxygen species, class III peroxidases may also contribute to the cross-linking of cell wall components, such as glycoproteins (Tenhaken 2015). The developing G-layer of phloem fibers from the tree *Mallotus japonicus* also shows a peroxidase activity, despite the

Fig. 11 Diagram of the assembly of the secondary cell wall in hemp bast fibers during the transition from phase H9 to phase H20. The middle lamella (ML), primary cell wall (PCW), S1 layer and G layer (the latter sometimes called tertiary cell wall) are indicated. Two different steps of assembly of the G layer are also indicated, respectively, the Gf layer (observed in H9) and the Gn layer (observed in H20). *PM* plasma membrane. The main protein and polysaccharide components analyzed in this work are indicated by symbols, explained in the legend
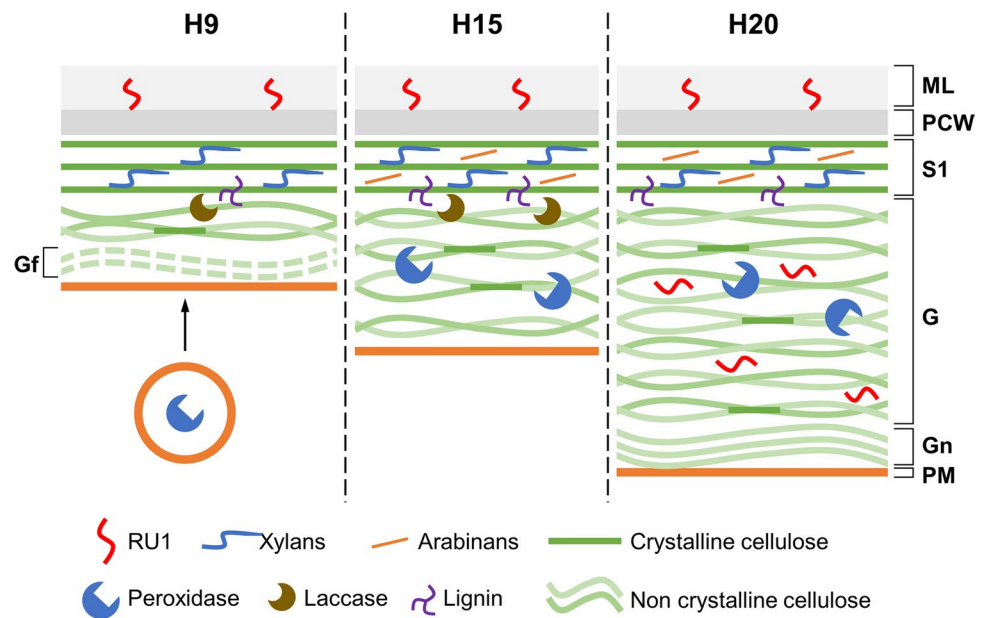
absence of lignin (Nakagawa et al. 2014). The presence of a CsaPRX64 signal in the cell cytoplasm in H9 suggests that the enzyme is secreted during the transition from H9 to H15 and then it accumulates in the G-layer, possibly modifying its organization. The functions of peroxidases found in the G-layer await further characterization.

Laccases are oxidative enzymes that are widely distributed in plants, fungi and bacteria, where they catalyze the oxidation of various phenolic and non-phenolic compounds. The distribution of laccase in hemp bast fibers must be interpreted with caution. The immunoelectron microscopy signal suggests that the enzyme is involved in biochemical processes intrinsic in the G-layer that is more in contact with the S1-layer (Fig. 10). The enzyme already accumulates in developing cell walls at H9, but, more considerably, at H15. At this developmental stage, the enzyme accumulates near the S1-layer. This indicates that the enzyme may be necessary for the progressive lignification occurring at the interface between S1- and G-layer. The role of laccase would culminate in H20, where the enzyme is distributed more uniformly in the G-layer; in addition, its relative quantity greatly decreases. The data in the literature suggest the importance of laccases during SCW development. In cotton, laccases play important roles in cell expansion and lignification. This is supported by the high number of genes coding for laccases expressed in cotton (several tens), many of which are expressed during the development of cotton fibers. The enzymatic activity of laccases is related to the higher content of lignin at 25 DPA (days post-anthesis) (Balasubramanian et al. 2016). In flax, the analysis of genes involved in the biosynthesis of lignin indicated that the multigene family of laccase plays important roles in the polymerization of monolignols and, therefore, in the production of lignin.

In addition, it is now known that the post-transcriptional regulation of gene activity is regulated by specific miRNAs (Le Roy et al. 2017). A precise control of both synthesis and deposition of lignin is clearly important to promote proper functioning of cells. For example, during the development of tracheal protoxylem in *Arabidopsis*, the deposition of lignin is specifically limited to SCWs to preserve the plasticity of PCWs. While the enzymes that synthesize monolignols have a uniform distribution during the differentiation of tracheal protoxylem, the laccases LAC4 and LAC17 are conversely localized in the SCW during differentiation (Schuetz et al. 2014). This finding reinforces the assumption that the exact delivery of oxidative enzymes determines the lignification of cell walls. Therefore, an exact localization of laccases is clearly expected and important during the development of both the S1- and G-layers of hemp bast fibers.

Conclusions

In conclusion, our study provides a fine mapping of pectic epitopes, xylan, crystalline cellulose, a class III peroxidase and a laccase. A model is here proposed to explain the results reported (Fig. 11). The data shown provide a visual analysis of the dynamics accompanying the transition of the hemp hypocotyl from elongation to thickening, previously revealed using RNA-Seq (Behr et al. 2016). Our ultrastructural analysis discloses morphological features underlying the G-layer remodeling, by confirming the previously reported "stripped" Gn-layer (Chernova et al. 2018) and by showing, for the first time, the existence of a "loose" cellulosic layer (Gf) at young developmental stages of the hemp hypocotyl.

References

Andeme-Onzighi C, Douchiche O, Driouich A, Morvan C (2005) Composition of flax hypocotyl fibres. J Nat Fibers 2:1–14. https://doi.org/10.1300/J395v02n03_01

Andersen MCF, Boos I, Marcus SE, Kračun SK, Rydahl MG, Willats WGT, Knox JP, Clausen MH (2016) Characterization of the LM5 pectic galactan epitope with synthetic analogues of β-1,4-D-galactotetraose. Carbohydr Res 436:36–40. https://doi.org/10.1016/J.CARRES.2016.10.012

Andre CM, Hausman JF, Guerriero G (2016) *Cannabis sativa*: the plant of the thousand and one molecules. Front Plant Sci 7:19

Balasubramanian VK, Rai KM, Thu SW, Hii MM, Mendu V (2016) Genome-wide identification of multifunctional laccase gene family in cotton (*Gossypium* spp.); expression and biochemical analysis during fiber development. Sci Rep 6:34309

Behr M, Legay S, Zizkova E, Motyka V, Dobrev PI, Hausman JF, Lutts S, Guerriero G (2016) Studying secondary growth and bast fiber development: the hemp hypocotyl peeks behind the wall. Front Plant Sci 7:1733

Behr M, Lutts S, Hausman J-F, Guerriero G (2018a) Expression analysis of cell wall-related genes in *Cannabis sativa*: the "ins and outs" of hemp stem tissue development. Fibers 6:27. https://doi.org/10.3390/fib6020027

Behr M, Sergeant K, Leclercq CC, Planchon S, Guignard C, Lenouvel A, Renaut J, Hausman JF, Lutts S, Guerriero G (2018b) Insights into the molecular regulation of monolignol-derived product biosynthesis in the growing hemp hypocotyl. BMC Plant Biol 18:1. https://doi.org/10.1186/s12870-017-1213-1

Berni R, Luyckx M, Xu X, Legay S, Sergeant K, Hausman J-F, Lutts S, Cai G, Guerriero G (2019) Reactive oxygen species and heavy metal stress in plants: impact on the cell wall and secondary metabolism. Environ Exp Bot 161:98–106. https://doi.org/10.1016/j.envexpbot.2018.10.017

Bhandari S, Fujino T, Thammanagowda S, Zhang D, Xu F, Joshi CP (2006) Xylem-specific and tension stress-responsive coexpression of KORRIGAN endoglucanase and three secondary wall-associated cellulose synthase genes in aspen trees. Planta 224:828–837

Blake AW, McCartney L, Flint JE, Bolam DN, Boraston AB, Gilbert HJ, Knox JP (2006) Understanding the biological rationale for the diversity of cellulose-directed carbohydrate-binding modules in prokaryotic enzymes. J Biol Chem 281:29321–29329. https://doi.org/10.1074/jbc.M605903200

Blake AW, Marcus SE, Copeland JE, Blackburn RS, Knox JP (2008) In situ analysis of cell wall polymers associated with phloem fibre cells in stems of hemp, *Cannabis sativa* L. Planta 228:1–13

Chernova TE, Gur'yanov OP, Brach NB, Pavlov AV, Porokhovinova EA, Kutuzova SN, Chemikosova SB, Gorshkova TA (2007) Variability in the composition of tissue-specific galactan from flax fibers. Russ J Plant Physiol 54:782–789

Chernova TE, Mikshina PV, Salnikov VV, Ibragimova NN, Sautkina OV, Gorshkova TA (2018) Development of distinct cell wall layers both in primary and secondary phloem fibers of hemp (*Cannabis sativa* L.). Ind Crops Prod 117:97–109

Christiernin M, Ohlsson AB, Berglund T, Henriksson G (2005) Lignin isolated from primary walls of hybrid aspen cell cultures indicates significant differences in lignin structure between primary and secondary cell wall. Plant Physiol Biochem 43:777–785

Crônier D, Monties B, Chabbert B (2005) Structure and chemical composition of bast fibers isolated from developing hemp stem. J Agric Food Chem 53:8279–8289. https://doi.org/10.1021/jf051253k

El-Tantawy A-A, Solís M-T, Da Costa ML, Coimbra S, Risueño M-C, Testillano PS (2013) Arabinogalactan protein profiles and distribution patterns during microspore embryogenesis and pollen development in *Brassica napus*. Plant Reprod 26:231–243. https://doi.org/10.1007/s00497-013-0217-8

Fike J (2016) Industrial hemp: renewed opportunities for an ancient crop. CRC Crit Rev Plant Sci 35:406–424

Francoz E, Ranocha P, Nguyen-Kim H, Jamet E, Burlat V, Dunand C (2015) Roles of cell wall peroxidases in plant development. Phytochemistry 112:15–21. https://doi.org/10.1016/j.phytochem.2014.07.020

Gorshkova T, Morvan C (2006) Secondary cell-wall assembly in flax phloem fibres: role of galactans. Planta 223:149–158

Gorshkova TA, Chemikosova SB, Sal'nikov VV, Pavlencheva NV, Gur'janov OP, Stolle-Smits T, van Dam JEG (2004) Occurrence of cell-specific galactan is coinciding with bast fiber developmental transition in flax. Ind Crops Prod 19:217–224

Gorshkova T, Chernova T, Mokshina N, Ageeva M, Mikshina P (2018) Plant "muscles": fibers with a tertiary cell wall. New Phytol 218:66–72

Goudenhooft C, Siniscalco D, Arnould O, Bourmaud A, Sire O, Gorshkova T, Baley C, Goudenhooft C, Siniscalco D, Arnould O, Bourmaud A, Sire O, Gorshkova T, Baley C (2018) Investigation of the mechanical properties of flax cell walls during plant development: the relation between performance and cell wall structure. Fibers 6:6. https://doi.org/10.3390/fib6010006

Guerriero G, Sergeant K, Hausman JF (2013) Integrated-omics: a powerful approach to understanding the heterogeneous lignification of fibre crops. Int J Mol Sci 14:10958–10978. https://doi.org/10.3390/ijms140610958

Guerriero G, Behr M, Backes A, Faleri C, Hausman JF, Lutts S, Cai G (2017) Bast fibre formation: insights from next-generation sequencing. Procedia Eng 200:229–235. https://doi.org/10.1016/j.proeng.2017.07.033

Guo K, Du X, Tu L, Tang W, Wang P, Wang M, Liu Z, Zhang X (2016) Fibre elongation requires normal redox homeostasis modulated by cytosolic ascorbate peroxidase in cotton (*Gossypium hirsutum*). J ExpBot 67:3289–3301

Gur'janov OP, Gorshkova TA, Kabel M, Schols HA, van Dam JEG (2007) MALDI-TOF MS evidence for the linking of flax bast fibre galactan to rhamnogalacturonan backbone. Carbohydr Polym 67:86–96

Hao Z, Mohnen D (2014) A review of xylan and lignin biosynthesis: foundation for studying *Arabidopsis irregular xylem* mutants with pleiotropic phenotypes. Crit Rev Biochem Mol Biol 49:212–241

Hernandez-Gomez MC, Rydahl MG, Rogowski A, Morland C, Cartmell A, Crouch L, Labourel A, Fontes CMGA, Willats WGT, Gilbert HJ, Knox JP (2015) Recognition of xyloglucan by the crystalline cellulose-binding site of a family 3a carbohydrate-binding

module. FEBS Lett 589:2297–2303. https://doi.org/10.1016/j.febslet.2015.07.009

Hernandez-Gomez MC, Runavot JL, Meulewaeter F, Knox JP (2017) Developmental features of cotton fibre middle lamellae in relation to cell adhesion and cell detachment in cultivars with distinct fibre qualities. BMC Plant Biol 17:69

His I, Andème-Onzighi C, Morvan C, Driouich A (2001) Microscopic studies on mature flax fibers embedded in LR white. J Histochem Cytochem 49:1525–1535. https://doi.org/10.1177/002215540104901206

Hobson N, Deyholos MK (2013) Genomic and expression analysis of the flax (*Linum usitatissimum*) family of glycosyl hydrolase 35 genes. BMC Genom 14:344. https://doi.org/10.1186/1471-2164-14-344

Iwai H, Terao A, Satoh S (2013) Changes in distribution of cell wall polysaccharides in floral and fruit abscission zones during fruit development in tomato (*Solanum lycopersicum*). J Plant Res 126:427–437

Jones L, Seymour GB, Knox JP (1997) Localization of pectic galactan in tomato cell walls using a monoclonal antibody specific to (1[→]4)-[beta]-ᴅ-galactan. Plant Physiol 113:1405–1412. https://doi.org/10.1104/pp.113.4.1405

Kiyoto S, Yoshinaga A, Fernandez-Tendero E, Day A, Chabbert B, Takabe K (2018) Distribution of lignin, hemicellulose, and arabinogalactan protein in hemp phloem fibers. Microsc Microanal 24:442–452. https://doi.org/10.1017/S1431927618012448

Le Roy J, Blervacq A-S, Créach A, Huss B, Hawkins S, Neutelings G (2017) Spatial regulation of monolignol biosynthesis and laccase genes control developmental and stress-related lignin in flax. BMC Plant Biol 17:124. https://doi.org/10.1186/s12870-017-1072-9

Lee KJD, Sakata Y, Mau S-L, Pettolino F, Bacic A, Quatrano RS, Knight CD, Knox JP (2005) Arabinogalactan proteins are required for apical cell extension in the moss *Physcomitrella patens*. Plant Cell 17:3051–3065. https://doi.org/10.1105/tpc.105.034413

Lee C, Teng Q, Zhong R, Ye ZH (2011) The four *Arabidopsis REDUCED WALL ACETYLATION* genes are expressed in secondary wall-containing cells and required for the acetylation of xylan. Plant Cell Physiol 52:1289–1301

MacMillan CP, Mansfield SD, Stachurski ZH, Evans R, Southerton SG (2010) Fasciclin-like arabinogalactan proteins: specialization for stem biomechanics and cell wall architecture in *Arabidopsis* and *Eucalyptus*. Plant J 62:689–703. https://doi.org/10.1111/j.1365-313X.2010.04181.x

McCartney L, Marcus SE, Knox JP (2005) Monoclonal antibodies to plant cell wall xylans and arabinoxylans. J Histochem 53:543–546

Mellerowicz EJ, Gorshkova TA (2012) Tensional stress generation in gelatinous fibres: a review and possible mechanism based on cell-wall structure and composition. J Exp Bot 63:551–565. https://doi.org/10.1093/jxb/err339

Mikshina P, Chernova T, Chemikosova S, Ibragimova N, Mokshina N, Gorshkova T (2013) Cellulosic fibers: role of matrix polysaccharides in structure and function. In: Van De Ven TGM (ed) Cellulose-fundamental aspects. InTech, Rijeka

Mikshina PV, Petrova AA, Gorshkova TA (2015) Functional diversity of rhamnogalacturonans I. Russ Chem Bull 64:1014–1023. https://doi.org/10.1007/s11172-015-0970-y

Mollard A, Joseleau J-P (1994) Acacia senegal cells cultured in suspension secrete a hydroxyproline-deficient arabinogalactan-protein. Plant Physiol Biochem 32:703–709

Nakagawa K, Yoshinaga A, Takabe K (2014) Xylan deposition and lignification in the multi-layered cell walls of phloem fibres in *Mallotus japonicus* (*Euphorbiaceae*). Tree Physiol 34:1018–1029. https://doi.org/10.1093/treephys/tpu061

Novo-Uzal E, Fernandez-Perez F, Herrero J, Gutierrez J, Gomez-Ros LV, Bernal MA, Diaz J, Cuello J, Pomar F, Pedreno MA (2013) From *Zinnia* to *Arabidopsis*: approaching the involvement of peroxidases in lignification. J ExpBot 64:3499–3518

Printz B, Dos Santos Morais R, Wienkoop S, Sergeant K, Lutts S, Hausman J-F, Renaut J (2015) An improved protocol to study the plant cell wall proteome. Front Plant Sci 6:237. https://doi.org/10.3389/fpls.2015.00237

Ralet M-C, Tranquet O, Poulain D, Moïse A, Guillon F (2010) Monoclonal antibodies to rhamnogalacturonan I backbone. Planta 231:1373–1383. https://doi.org/10.1007/s00425-010-1116-y

Rennie EA, Scheller HV (2014) Xylan biosynthesis. Curr Opin Biotechnol 26:100–107

Reynolds ES (1963) The use of lead citrate at high pH as an electron-opaque stain in electron microscopy. J Cell Biol 17:208

Reza M, Kontturi E, Jääskeläinen AS, Vuorinen T, Ruokolainen J (2015) Transmission electron microscopy for wood and fiber analysis – A review. BioResources 10:6230–6261

Roach MJ, Mokshina NY, Badhan A, Snegireva AV, Hobson N, Deyholos MK, Gorshkova TA (2011) Development of cellulosic secondary walls in flax fibers requires beta-galactosidase. Plant Physiol 156:1351–1363

Ruel K, Nishiyama Y, Joseleau JP (2012) Crystalline and amorphous cellulose in the secondary walls of *Arabidopsis*. Plant Sci 193:48–61

Ruprecht C, Bartetzko MP, Senf D, Dallabernadina P, Boos I, Andersen M, Kotake T, Knox JP, Hahn MG, Clausen M, Pfrengle F (2017) A synthetic glycan microarray enables epitope mapping of plant cell wall glycan-directed antibodies. Plant Physiol 175:1094–1104. https://doi.org/10.1104/pp.17.00737

Salnikov VV, Ageeva MV, Gorshkova TA (2008) Homofusion of Golgi secretory vesicles in flax phloem fibers during formation of the gelatinous secondary cell wall. Protoplasma 233:269–273. https://doi.org/10.1007/s00709-008-0011-x

Sanchez-Rodriguez C, Bauer S, Hematy K, Saxe F, Ibanez AB, Vodermaier V, Konlechner C, Sampathkumar A, Ruggeberg M, Aichinger E, Neumetzler L, Burgert I, Somerville C, Hauser M-T, Persson S (2012) CHITINASE-LIKE1/POM-POM1 and its homolog CTL2 are glucan-interacting proteins important for cellulose biosynthesis in *Arabidopsis*. Plant Cell 24:589–607. https://doi.org/10.1105/tpc.111.094672

Schuetz M, Benske A, Smith RA, Watanabe Y, Tobimatsu Y, Ralph J, Demura T, Ellis B, Samuels AL (2014) Laccases direct lignification in the discrete secondary cell wall domains of protoxylem. Plant Physiol 166:798–807

Snegireva A, Chernova T, Ageeva M, Lev-Yadun S, Gorshkova T (2015) Intrusive growth of primary and secondary phloem fibres in hemp stem determines fibre-bundle formation and structure. AoB Plants 7:plv061

Sorek N, Sorek H, Kijac A, Szemenyei HJ, Bauer S, Hématy K, Wemmer DE, Somerville CR (2015) The *Arabidopsis* COBRA protein facilitates cellulose crystallization at the plasma membrane. J Biol Chem 290:25274. https://doi.org/10.1074/jbc.A114.607192

Tenhaken R (2015) Cell wall remodeling under abiotic stress. Front Plant Sci 5:771

Willats WGT, Marcus SE, Knox JP (1998) Generation of a monoclonal antibody specific to (1→5)-α-ʟ-arabinan. Carbohydr Res 308:149–152. https://doi.org/10.1016/S0008-6215(98)00070-6

Publisher's Note Springer Nature remains neutral with regard to jurisdictional claims in published maps and institutional affiliations.